PRODUCTION AND COMPARATIVE STUDY OF ZnO FILMS OBTAINED BY MAGNETRON SPUTTERING, MOCVD AND ELECTROCHEMICAL DEPOSITION

E. Rusu[1], A. Burlacu[1], V. Zalamai[2], V. Ursaki[2], V. Prilepov[3]
[1)] Institute of Electronic Engineering and Nanotechnology „D. Ghițu" of the Academy of Sciences of Moldova, Academy str. 3/3, Chisinau MD-2028, Moldova
[2)] Institute of Applied Physics of the Academy of Sciences of Moldova, Academy str. 5, Chisinau MD-2028, Moldova
[3)] State University of Moldova, Mateevici str. 60, Chisinau MD-2009, Moldova
rusue@nano.asm.md

Abstract. *It was found that the morphology, electrical and luminescence properties of ZnO layers obtained by Magnetron sputtering, MOCVD and Electrochemical deposition can be controlled by technological parameters such as the ratio of argon-to-oxygen gases in the gas flow as well as the temperature of the substrate with the MOCVD and magnetron sputtering method, or by the composition and the temperature of solutions with the ECHD method. The low temperature PL spectra of nanorods grown by MOCVD is dominated by emission related to neutral donor bound excitons (D^0X), while the emission from nanodots is dominated by a band related to donor-acceptor DA recombination. The origin of the DA PL band is discussed. The low temperature PL spectrum of ZnO bulk layers in the near-bandgap spectral range is dominated by a superposition of D^0X related bands. The smooth films produced with a high Ar/O ratio during magnetron sputtering exhibit weak luminescence suggesting an amorphous nature of the film. Annealing of samples in air during 30 min at 450 ^oC after the deposition process leads to increasing luminescence intensity due to the crystallization.*

An n-ZnO/p-Si photodiode structure was produced by MOCVD, and its electrical characteristics were investigated in details.

Keywords: *ZnO films, nanorods, nanodots, Magnetron sputtering, MOCVD, Electrochemical deposition, photoluminescence spectroscopy.*

I. Introduction

The Zinc oxide is a promising material for diverse applications in optoelectronics, nanoelectronics, photonics, transparent electronics, hybrid electronics, and gas sensors [1]. Nanostructured ZnO and planar ZnO films can be produced by various methods such as metalorganic chemical vapor deposition (MOCVD), molecular beam epitaxy (MBE), chemical bath deposition (CBD), electrochemical deposition (ECHD), magnetron sputtering and other techniques [1,2].

Such methods as chemical, electrochemical, sol-gel, VLS, and chemical vapour transport and condensation growth are cost effective. However, they basically lead to the production of nanostructured layers, such as wires, rods, ribbons, belts, tubes, discs, tetrapods, combs, rings, springs, propeller arrays, etc, it being hard to produce smooth and flat layers with these techniques. Smooth and flat films are highly desired in homojunction and heterojunctions. Smooth surfaces can be obtained with MOCVD and MBE methods. However, these technologies are quite expensive. Magnetron sputtering is a technique which allows one to produce both nanostructured and flat layers, in being at the same time less expensive than MOCVD and MBE technologies.

In this work, we investigate the morphology and the photoluminescence (PL) properties of

ZnO layers produced by MOCVD, magnetron stuttering, and ECHD in order to establish their dependence upon the technological conditions of growth.

II. Experimental details

In the MOCVD growth, ZnO layers were produced in a horizontal double furnace set-up consisting of a source furnace and a main furnace. Zinc acetylacetonate hydrate (Aldrich) loaded into a quartz boat was used as source material introduced into the source furnace. The vapors were transported into the main furnace by Ar gas flow which was mixed with another flow of Ar and O_2 gases at the entrance of the main furnace. The source material was maintained at 130 ^oC, while the temperature of the Si or glass substrates in the main furnace was set at 500 ^oC. The deposition process was carried out for 1 h. The morphology of the produced ZnO structures was determined by the ratio of the gas flow rates.

Magnetron sputtering of ZnO films was performed in an installation assembled on the basis of a VUP-5 instrument. A control sample was placed in the stuttering chamber near the Si, SiO_2/Si, or ITO-on-glass basic support for monitoring the deposition process via measuring the resistivity of the layer deposited on the control sample. A 99,99 % purity Zn plate with a diameter of 40 mm and thickness of 5 mm doped with 2% wt of Al was used as target. The temperature of both the control and the basic supports was maintained at a temperature from the interval 200 – 220 ^oC, while the magnetron power was W=360 V x 100 mA. The Si support was treated in a 30% $Na_2S_2O_3x5H_2O$ solution before the sputtering process for improving the adhesion of the deposited ZnO layer. A mixture of Ar+O was used as working gas. The ratio of Ar/O in the gas flow was changed and air was introduced in the growth chamber for a certain period of time during the sputtering process in order to control the morphology and the radiative properties of the deposted ZnO film. The samples were annealed in air during 30 min at 450 ^oC after the deposition process.

The electrochemical deposition was performed from an electrochemical solution consisting of 0.4 mM zinc nitrate $Zn(NO_3)_2$ and 0.1 M hydrogen peroxide H_2O_2 with an Ag/AgCl reference electrode, a Pt counter electrode and a metallic Zn plate as a substrate working electrode. Zinc hydroxide ($Zn(OH)_2$) is formed as result of chemical reactions after the application of a cathodic potential. The hydroxide is transformed into zinc oxide which is deposited onto the cathode at temperatures above 60 ^oC.

A VEGA TESCAN TS 5130 MM scanning electron microscope (SEM) was used for morphological characterization of the samples.

Photoluminescence was excited by 325 nm line of a He-Cd Melles Griot laser and was analyzed through a double spectrometer at low temperature (10 K). The resolution was better than 0.5 meV. The samples were mounted on the cold station of a LTS-22-C-330 cryostat.

III. Morphology characterization

It was found that the morphology, electrical and luminescence properties of ZnO layers obtained by these methods can be controlled by technological parameters such as the ratio of argon-to-oxygen gases in the gas flow as well as the temperature of the substrate with the MOCVD and magnetron sputtering method, or by the composition and the temperature of solutions with the ECHD method.

Bulk ZnO layers with the thickness around 3 μm (Fig. 1c) are obtained with the MOCVD when a 140 sccm flow rate of the Ar carrier gas from the source is mixed with the second Ar + O_2 gas flow with the ratio of 50 sccm to 140 sccm. If the Ar carrier gas flow rate from the source is reduced to 40 sccm, ZnO nanorods or nanodots are produced depending on the ratio of flow rates in the second Ar + O_2 gas flow. ZnO nanorods with the morphology illustrated in Fig. 1b are produced

with the ratio of the argon to oxygen flow rates of 130 to 140 sccm. The nanorods are arrow-headed with a mean diameter of 200 – 400 nm. The height of nanorods is up to 1 μm. A layer of nanodots with a mean diameter of 100 nm illustrated in Fig. 1a is obtained when the ratio of the argon to oxygen flow rates is 50 to 140 sccm.

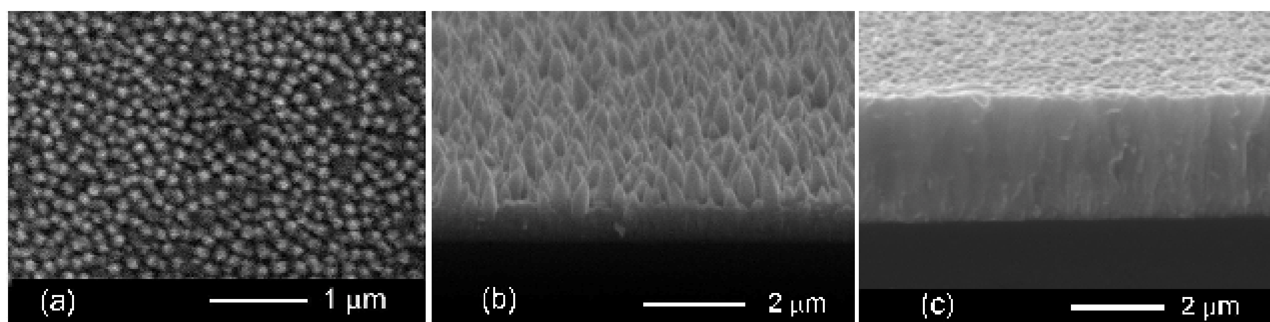

Fig. 1. SEM images taken from ZnO nanodots (a), nanorods (b) and bulk ZnO layers (c) grown by MOCVD.

The investigation of the morphology of ZnO layers grown by magnetron sputtering demonstrated that it is determined by the technological conditions such as the pressure of gases in the growth chamber, the concentration of oxygen, as well as by the substrate used. It was found that the introduction of air in the growth chamber for a period of time longer than 30 min during the sputtering process leads to the oxidation of the target. This oxidation, in turn, affects the magnetron power and creates instabilities in plasma maintaining. The velocity of gas flows into the chamber is set to a value assuring the maintenance of a constant pressure, and therefore a stability of the created plasma.

The morphology of the produced ZnO layers was found to be determined first of all by the ratio of argon to oxygen gases in the gas flow during the growth process. High values of the Ar/O ratio result in the production of smooth and flat ZnO films. The increase of the oxygen content into the gas flow leads to the production of porous layers as shown in Fig. 2a and 2b. When the Ar:O ratio is 1:1, the obtained ZnO layer consists of microcrystallites as shown in Fig. 2a. The size of these crystallites is around 200 – 500 nm. Further increase of the oxygen content leads to the creation of spectacularly twisted microstructures (Fig. 2b) which prove to be porous at a more accurate analysis. The length of the microstructures produced with an Ar:O ratio of 1:10 on an ITO-on-glass substrate vary in the range of 4 to 20 μm with a diameter of 1 – 4 μm.

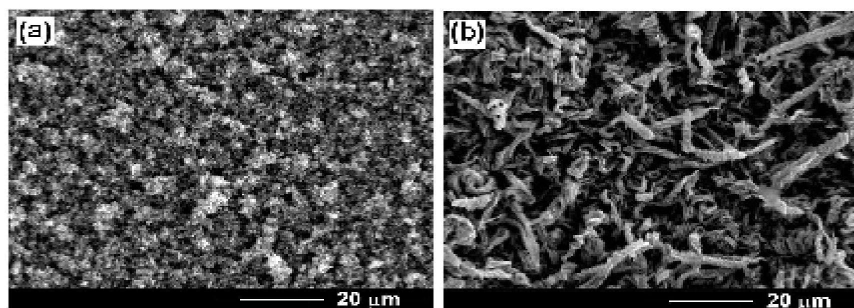

Fig. 2. SEM image of ZnO layers produced by magnetron sputtering in processes with different ratio of argon to oxygen gases in the gas flow during the growth process as follows: Ar:O = 1:1 (a); Ar:O = 1:10 (b).

Electrochemical deposition is an inexpensive a versatile method for the preparation of a variety of morphologies ranging from nanorods as shown in Fig. 3 (left) to complex assemblies as demonstrated in the right sections of Fig. 3.

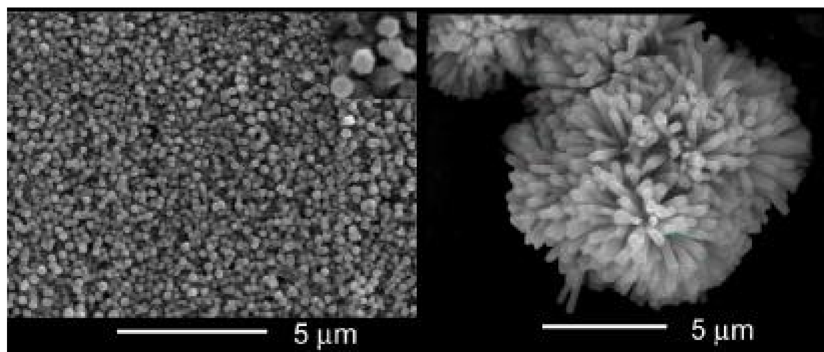

Fig. 3. SEM image of ZnO structures produced by electrodeposition.

IV. Photoluminescence analysis

Apart from morphology, the technological parameters strongly influence the radiative properties of the produced ZnO layers. The low temperature PL spectra of nanorods grown by MOCVD with the morphology illustrated in Fig. 1b is dominated by emission related to neutral donor bound excitons (D^0X) accompanied by LO replica, while the donor-acceptor (DA) emission is at least two orders of magnitude weaker (Fig. 4, curve 2). Three D^0X related lines are resolved in the spectrum at 3.371; 3.363; 3.360 eV, which correspond to previously reported I_1, I_4, and I_8 lines (see, e.g., [3,4]).

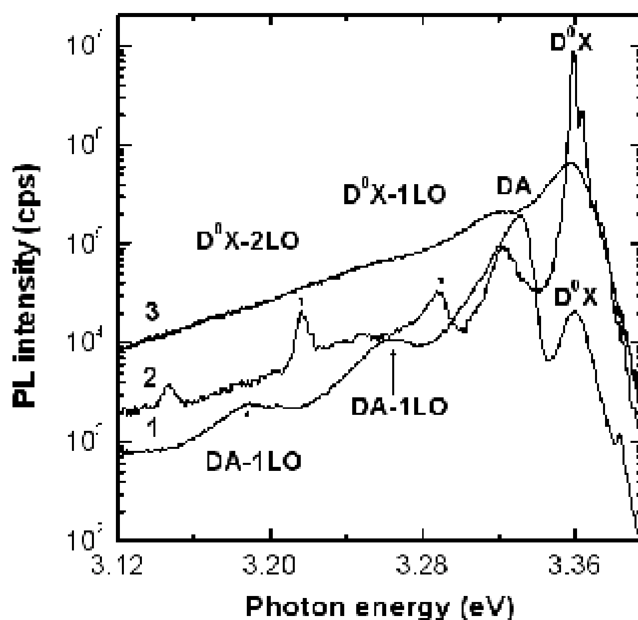

Fig. 4. PL spectra at T = 10 K of nanodots (curve 1), nanorods (curve 2), and bulk ZnO layers (curve 3) grown by MOCVD.

In contrast to the PL spectra of ZnO nanorods, the low temperature emission from nanodots with the morphology illustrated in Fig. 1a is dominated by a band with the maximum at 3.33 eV suggested to be related to DA recombination (Fig. 4, curve 1). The intensity of the DA band sharply decreases with increasing temperature, since the impurity with smaller binding energy involved in DA transitions (most probably the donor impurity) is ionized with increasing temperature. As concerns the acceptor involved in DA recombination, it is most probably related to zinc vacancy. It was

previously shown that V_{Zn} is a relevant defect in ZnO [5]. Positron annihilation experiments identified the Zn vacancy as the dominant defect in ZnO [6-10]. It is believed that the Zn vacancy energy level is positioned approximately 3.06 eV below the conduction band edge [11,12]. From the energy position of the PL band (3.33 eV), one can suggest that this band is related to a [V_{zn}-X] complex [10] rather than to an isolated V_{Zn} defect. The density of a defect with the estimated ionization energy of 90 – 120 meV has been correlated to the concentration of Zn vacancies in ZnO films on the basis of PL and positron annihilation spectroscopy analysis [9]. This ionization energy is in a good correlation with the position of the 3.33 eV PL band in our nanodot samples. Positron annihilation spectroscopy in heteroepitaxial ZnO films grown by MOCVD demonstrated a high concentration of V_{Zn} defects close to the interface, and the decrease of their concentration with increasing the distance from the interface [8]. This observation explains the high intensity of the 3.33 eV PL band in small ZnO nanodots situated close to the interface with the substrate, and the low intensity of this band in ZnO nanorods.

The low temperature PL spectrum of ZnO bulk layers in the near-bandgap spectral range is dominated by a superposition of D^0X related bands (Fig. 4, curve 3.).

Similarly to samples grown with MOCVD, the ratio of argon to oxygen gases in the gas flow during the magnetron sputtering process strongly influences the radiative properties of the produced ZnO layers. The smooth films produced with a high Ar/O ratio exhibit weak luminescence suggesting an amorphous nature of the film. Annealing of samples in air during 30 min at 450 ^oC after the deposition process leads to increasing luminescence intensity due to the crystallization. The near-band-edge luminescence at 10 K is dominated by two bands at 3.61 and 3.71 eV related to the recombination of donor bound excitons (D^0X) (curve 1 in Fig. 5).

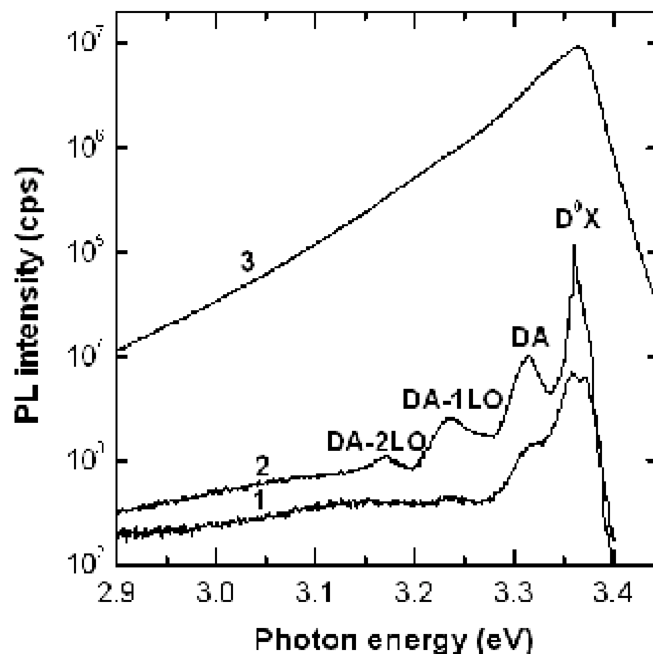

Fig. 5. PL spectra of ZnO layers produced by magnetron sputtering in processes with different ratio of argon to oxygen gases in the gas flow during the growth process as follows: Ar:O = 10:1 (curve 1); Ar:O = 1:1 (curve 2); Ar:O = 1:10 (curve 3). The samples were annealed in air during 30 min at 450 ^oC after the deposition process.

The D^0X bands at 3.61 eV and 3.71 eV correspond to the previously observed I_1 and I_6 bands, the I_6 band being associated with the Al impurity [3]. Apart from the D^0X bands, a PL band is observed at 3.314 eV accompanied by LO phonon replicas, it being previously attributed to the donor-acceptor pair recombination (DA) [13].

The increase of the oxygen content in the Ar/O ratio to 1:1 leads to the intensification of the near-band-edge luminescence by an order of magnitude, the D^0X band related to the Al impurity becoming highly predominant (Fig. 5, curve 2) suggesting an efficient optical activation of this impurity.

Further increase of the oxygen content leads to a spectacular increase of the near-band-edge luminescence intensity by additional several orders of magnitude with a concomitant broadening of the near-band-edge luminescence band. A characteristic feature of this PL band is the broadening toward the Stokes part of the emission. The width of this PL band is 58 meV at 10 K. It was previously shown that most probably this PL band is due to direct transitions of electrons from the conduction band tails to valence band tails [14]. The broadening of the PL band involved can be accounted for by the broadening of the band edges due to potential fluctuations induced by the high concentration of intrinsic defects or impurities. This model has been applied to correlate the width of the PL band to the free carrier concentration in highly doped ZnO samples [14]. By using the established dependence, one can estimate that the electron concentration in the sample produced with the Ar:O ratio of 1:10 is 4.0×10^{19} cm^{-3} at T = 10 K. These data suggest that increasing the oxygen content in the Ar/O ratio during the magnetron sputtering promotes the optical and electrical activation of the doping Al impurity.

As concerns the samples prepared by electrodeposition, one should mention that their optical quality is lower as compared to samples prepared by MOCVD and magnetron sputtering. The low temperature luminescence intensity in these samples is by 3 orders of magnitude lower as compared to samples prepared by MOCVD and magnetron sputtering (Fig. 6). Similarly to samples produced by magnetron sputtering with the Ar:O ratio of 1:10, the near-band-gap PL band in samples prepared by electrodeposition is broadened towards the Stokes part of the emission. As discussed above, the broadening of the PL band involved can be accounted for by the broadening of the band edges due to the potential fluctuations induced by the high concentration of intrinsic defects.

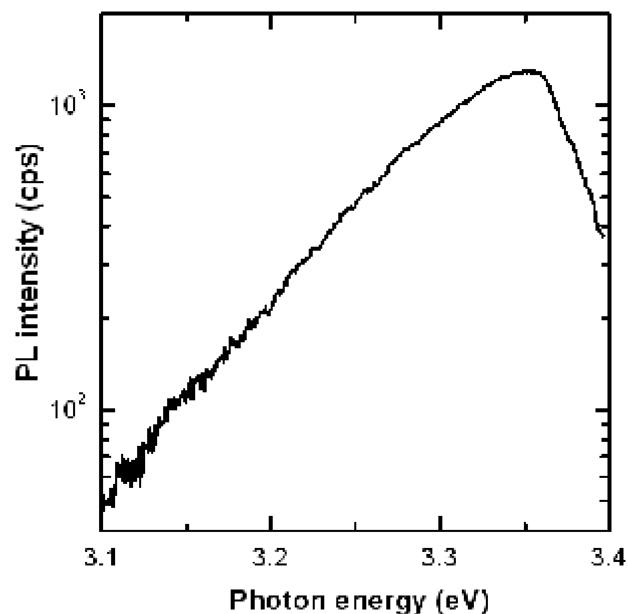

Fig. 6. PL spectrum of ZnO layers produced by electrodeposition.

V. Electrical characterization of the n-ZnO/p-Si heterostructure

An n-ZnO/p-Si photodiode structure was produced by MOCVD deposition. The current-voltage characteristics of this heterostructure in linear and logarithmic scale are presented in Fig. 7.

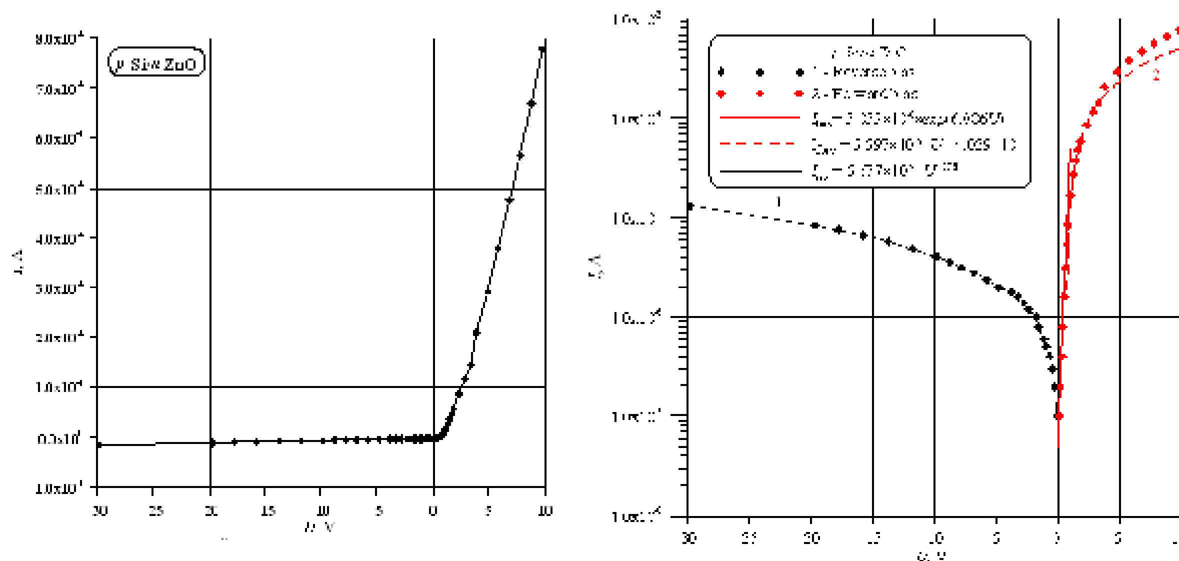

Fig. 7. Current-voltage characteristic of the n-ZnO/p-Si heterojunction in a linear and a logarithmic scale.

The forward current-voltage characteristic in the region of low bias (0.1 – 0.6 V) is well described by the relation I_{forv}=5.053·10^{-8}·exp(6.886U), which corresponds to a diode coefficient of n=5.76. This value is characteristic to a tunneling or to many-step tunneling-recombination transport mechanism [15-17]. The forward current-voltage characteristic in the region of bias between 1 V and 3.5 V is described by a linear dependence I_{forv} = 5,597·10^{-5}·U - 4.029·10^{-5} with a cut-off voltage of U_0 =0.72 V, and a resistance R_0=1.787·10^4Ω.

$$I_0 = \frac{U - U_0}{R_0}.$$

Above the bias of 4.0V, the characteristic follows a super-linear power type dependence I_{forv}=3.335·10^{-5}·$U^{1.379}$, while the reverse characteristic in the region of bias of 0 – 10 V reveals a sub-linear dependence I_{rev}=5.677·10^{-7}·$U^{0.821}$.

VI. Conclusions

The morphology, electrical and luminescence properties of ZnO layers obtained by Magnetron sputtering, MOCVD and Electrochemical deposition are controlled by technological parameters. Bulk ZnO layers, ZnO nanorods or nanodots are produced depending on the ratio of flow rates in the Ar + O_2 gas flow in the MOCVD furnace.

The morphology of the produced ZnO layers produced by magnetron sputtering is determined first of all by the ratio of argon to oxygen gases in the gas flow during the growth process. High values of the Ar/O ratio result in the production of smooth and flat ZnO films. The increase of the oxygen content into the gas flow leads to the production of porous layers. When the Ar:O ratio is 1:1, the obtained ZnO layer consists of microcrystallites with sizes around 200 – 500 nm. Further increase of the oxygen content leads to the creation of spectacularly twisted microstructures which prove to be porous.

The low temperature PL spectra of nanorods grown by MOCVD is dominated by emission related to neutral donor bound excitons (D^0X), while the emission from nanodots is dominated by a band related to donor-acceptor DA recombination. The acceptor involved in DA recombination is most probably related to zinc vacancy in a [V_{zn}-X] complex. The high intensity of the DA PL band

in small ZnO nanodots situated close to the interface with the substrate, and the low intensity of this band in ZnO nanorods is explained by a high concentration of V_{Zn} defects close to the interface, and the decrease of their concentration with increasing the distance from the interface. The low temperature PL spectrum of ZnO bulk layers in the near-bandgap spectral range is dominated by a superposition of D^0X related bands.

The smooth films produced with a high Ar/O ratio during magnetron sputtering exhibit weak luminescence suggesting an amorphous nature of the film. Annealing of samples in air during 30 min at 450 ^oC after the deposition process leads to increasing luminescence intensity due to the crystallization. The increase of the oxygen content in the Ar/O ratio leads to a spectacular increase of the near-band-edge luminescence intensity which suggests that optical and electrical activation of the doping Al impurity occurs.

The analysis of the current-voltage characteristic of n-ZnO/p-Si heterojunction structure produced by MOCVD suggests that the transport mechanism in this structure is determined by tunneling or by many-step tunneling-recombination process.

VII. References

1. I. M. Tiginyanu, O. Lupan, V. V. Ursaki, L. Chow, M. Enachi, Nanostructures of Metal Oxides, in Comprehensive Semiconductor Science and Technology, Chapter 3.11, pp. 396-479 (2011).
2. V. V. Ursaki, E. V. Rusu, A. Sarua, M. Kuball, G. I. Stratan, A. Burlacu, I. M. Tiginyanu, Nanotechnology, vol. 18, 215705 (2007).
3. B. K. Meyer B K et al., Phys. Stat. Sol. (b), vol. 241**,** 231 (2004).
4. V. V. Ursaki, I. M. Tiginyanu, V. V. Zalamai, et al., Phys. Rev. B , vol. 70 155204 (2004).
5. A. F. Kohan, G. Ceder, D. Morgan, C. G. Van de Walle, Phys. Rev. B, vol. 61**,** 15019 (2000).
6. F. Tuomisto, V. Ranki, K. Saarinen, D. C. Look, Phys. Rev. Lett. Vol. 91, 205502 (2003).
7. J. Zhong, A. H. Kitai, P. Mascher, W. Puff, J. Electrochem. Soc.**,** vol. 140, 3644 (1993).
8. A. Zubiaga, F. Tuomisto, F. Plazaola, K. Saarinen, J. A. Garcia, J F. Rommeluere, J. Zuñiga-Pérez, V. Muñoz-Sanjosé, Appl. Phys. Lett. Vol. 86, 042103 (2005).
9. A. Zubiaga, J. A. García, F. Plazaola, F. Tuomisto, K. Saarinen, J. Zuñiga Pérez, V. Muñoz-Sanjosé, J. Appl. Phys., vol. 99, 053516 (2006).
10. A. Zubiaga, F. Plazaola, J. A. García, F. Tuomisto, V. Muñoz-Sanjosé, R. Tena-Zaera, Phys. Rev. B, vol. 76, 085202 (2007).
11. B. Lin, Z. Fu, Y. Jia, Appl. Phys. Lett., vol. 79, 943 (2001).
12. S. H. Jeong, B. S. Kim, B. T. Lee, Appl. Phys. Lett., vol. 82, 2625 (2003).
13. V. V. Ursaki, I. M. Tiginyanu, V. V. Zalamai, V. M. Masalov, E. N. Samarov, G. A. Emelcenko, F. Briones, Semiconductor Science and Technology, vol. 19, 851 (2004).
14. V. V. Zalamai, V. V. Ursaki, E. Rusu, P. Arabadji, I. M. Tiginyanu, L. Sirbu, Appl. Phys. Lett., vol. 84, 5168 (2004).
15. S. M. Sze. Physics of Semiconductor Devices, John Wiley & Sons Inc, 1981.
16. A. G. Milnes, D. L. Feucht. Heterojunctions and metal-semiconductor junctions. Academic Press, 1972.
17. B. L. Sharma, R. K. Purohit. Semiconductor heterojunctions. Pergamon Press, 1974.